STUDIES OF MULTIPACTING IN AXISYMMETRIC CAVITIES FOR MEDIUM-VELOCITY BEAMS*

W. Hartung
National Superconducting Cyclotron Lab, Michigan State University, East Lansing, Michigan
F. Krawczyk
Los Alamos National Laboratory, Los Alamos, New Mexico
H. Padamsee
Laboratory of Nuclear Studies, Cornell University, Ithaca, New York

Abstract

A number of superconducting cavities of axisymmetric geometry have been designed to accelerate "medium-velocity" beams (β between 0.4 and 1, where β is the particle velocity divided by c). The medium-velocity cavities must be free of multipacting in order to achieve the desired performance. Simulations were done to assess the risk of multipacting in medium-velocity cavities developed for the Accelerator Production of Tritium (APT) project, the Spallation Neutron Source (SNS), and the Rare Isotope Accelerator (RIA). The predictions are compared to the results of the first few RF tests on prototype cavities.

1 INTRODUCTION

Multipacting can limit the performance of an SRF cavity: the electromagnetic energy accelerates secondary electrons, which strike the cavity wall and produce more secondary electrons, in a self-sustaining process. The electron bombardment produces heat, reducing the Q. If additional power is supplied, more secondary electrons are generated, so that the Q drops further, without any increase in field.

Multipacting was a performance limit for the first superconducting RF accelerator at Stanford [1]. It was also a problem for the "muffin tin" cavities developed at Cornell [2]. Multipacting is also seen in RF couplers, near RF windows, in coaxial lines, and in normal conducting cavities.

For superconducting cavities, experience indicates that the best cure is to choose a cell shape that inhibits multipacting. With the switch from flat walls (pillbox or muffin tin geometry) to a spherical or elliptical shape, multipacting has been mostly eliminated. However, in the design of a new cavity geometry, multipacting is a major concern.

Multipacting was of especial concern when the first cavities for acceleration of medium-velocity beams were designed. Three multi-cell cavity geometries at 700 MHz were designed for the APT project at Los Alamos [3, 4]. The cavities have $\beta_g = 0.48$, 0.64, and 0.82, where β_g is the geometrical β. More recently, different geometries at 805 MHz have been devised to cover similar β_g values for SNS [5] and RIA [6].

Simulations were done for these 6 cavity geometries to predict whether multipacting will be a problem. The cell shapes are shown in Figure 1. The simulation results will be reported in this paper and compared to the cold tests on the first few prototype single- and multi-cell cavities for APT, SNS, and RIA. A single-cell geometry was used for all of the simulations. The results will also be compared to predictions from other simulation codes.

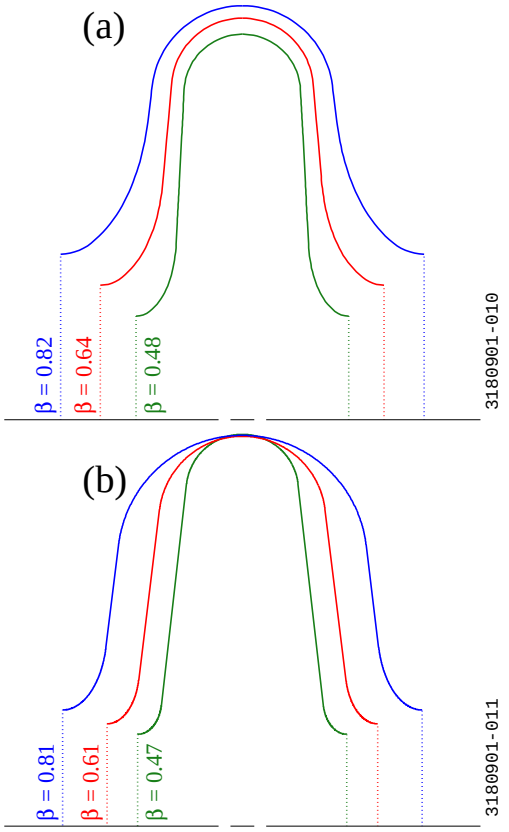

Figure 1. Cell shapes for (a) APT cavities and (b) SNS and RIA cavities (all scaled to the same frequency).

2 MULTIPACTING PHENOMENA

An electron hitting a surface can knock out electrons from the material via secondary emission [7, 8]. Electrons are also produced via reflection and back-scattering, although these effects are not considered herein. The secondary emission yield (SEY) = δ is defined as the number of secondary electrons produced by 1 incident electron. If $\delta > 1$, it is in principle possible to have an unbridled multiplication of electrons.

The SEY depends on the kinetic energy (K) of the in-

*Work supported by the National Science Foundation, the Department of Energy, and Michigan State University.

cident electron. For large K, the SEY also depends on the angle α (measured relative to the surface normal) at which the electron strikes the surface. Moreover, the SEY depends strongly on the condition of the surface, so there is no unique $\delta(K,\alpha)$ function for a given material. However, a generic $\delta(K)$ curve for normal incidence is shown in Figure 2. Generally, the SEY begins to depend on α for $K > K_p$, with δ increasing as α increases.

To sustain multipacting in a cavity, we need (i) to have electron trajectories which repeat, and (ii) a combination of impact energy K and impact angle α in the dangerous range, where δ might be ≥ 1. For (i), typically, the time between emission and impact must be an integer multiple of half the RF period. For (ii), the dangerous range is $K_1 < K < K_2$ (see Figure 2).

If the multipacting discharge cleans the surface and reduces δ, we can process through multipacting barriers. The effect of the processing would be to make the dangerous range for K smaller, *i.e.* to increase K_1 and decrease K_2. We cannot process through multipacting barriers that have K values in the most dangerous range. Some approximate values of K_1 and K_2 for Nb [9, 10] are given in Table 1.

3 SIMULATION TECHNIQUES

Simulations of multipacting in SRF cavities were done at Stanford [1] and Cornell [2]. Simulations have also been done at CERN, Wuppertal, DESY, and INFN. The most recent work was done by Helsinki, Saclay, and others. An overview of the subject was given at this workshop [11].

With the advances in computing speed and in sophistication of the simulation codes, the simulation of multipacting is becoming a practical design tool. The simulations described herein were done with a code that has been under development at Cornell for a number of years. The code has been expanded considerably over the years, although the basic electron tracking remains the same. The code was used in the past to simulate multipacting in muffin tin cavities [2] and CEBAF cavities [12]. Good agreement was found between the simulations and temperature mapping

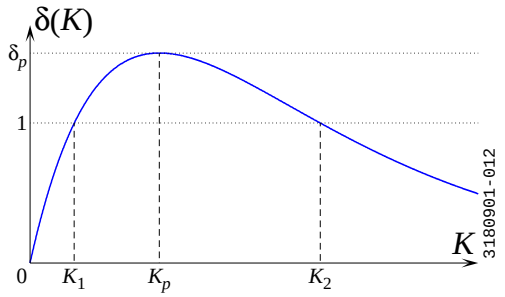

Figure 2. Generic dependence of SEY on kinetic energy.

Table 1. Approximate parameters for SEY curve of Nb.

Condition	K_1	K_2
high SEY	$\sim$ 27 eV	$\gtrsim$ 2000 eV
typical SEY	$\sim$ 40 eV	$\sim$ 1000 eV
low SEY	$\sim$ 150 eV	$\sim$ 750 eV

of single-cell CEBAF cavities [12].

Simulations have been done by P. Ylä-Oijala (Helsinki) for the RIA [13] and SNS [14] cavities. Some simulations for APT and SNS cavities were done by INFN-Genoa, albeit for different cell shapes than those used herein.

In what follows, E_p, K, α, and S are the peak surface electric field, electron kinetic energy, angle between the electron's velocity vector and the surface normal, and distance along the cavity surface from the equator, respectively. The i and f subscripts will refer to the initial (upon release of the secondary e^-) and final (at impact) values.

3.1 *Brute Force Method*

The following procedure was used:

- Select a cavity shape and a resonant mode.
- Compute the electromagnetic field distribution using SUPERFISH [15] or SuperLANS [16]. Initially we used SUPERFISH, then we switched to SuperLANS.
- Try different starting conditions, typically $\sim$ 80 positions, $\sim$ 100 phases, $\sim$ 1000 field levels, corresponding to about $8 \cdot 10^6$ combinations.
- The most probable initial condition is $K_i = 2$ eV and $\alpha_i = 0$ [8]. We looked at $K_i = 0$, 1, 2, and 3 eV for $\alpha_i = 0$, plus $\alpha_i = \pm 15°$ and $\pm 30°$ for $K_i = 2$ eV. Thus, we considered a total of 8 cases, corresponding to about $6 \cdot 10^7$ combinations, for each cell shape.
- Track electron trajectories via numerical solution of the equations of motion.
- Allow secondary emission if an electron hits the wall with 20 eV $< K_f <$ 3 keV (this K range is pessimistic, as it corresponds to K_1 and K_2 values for an unusually large SEY curve).
- Stop tracking if the impact energy is out of range, the RF phase is wrong (in the case of $K_i = 0$), or if the electron does not hit the wall after 100 RF periods.
- Identify pathological cases. Multipacting might occur if we can keep tracking for many generations (limit = 41 for most cases).

The final step is to infer the likelihood of multipacting barriers from the predicted K_f and α_f values. No explicit $\delta(K,\alpha)$ function is assumed in the simulation (since the exact function is not generally known), so this final step is done manually, as will be described below.

3.2 *EM Field Calculation*

The multipacting trajectories often remain very close to the wall, so an accurate electromagnetic field distribution near the cavity surface is essential. This was a source of difficulty with the EM field distributions from SUPERFISH: we found multipacting trajectories at the locations of artifacts in the EM field. SuperLANS gives a smoother field distribution; the surface electric fields near the equator are compared in Figure 3. We used the field distributions from SuperLANS as input to the multipacting simulations presented herein. Figure 4 shows the SuperLANS mesh and electric field lines for one of the cavities. The artifacts in the SUPERFISH field require closer scrutiny—they may

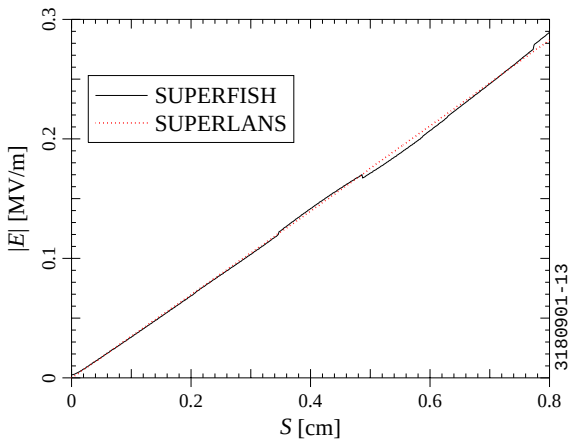

Figure 3. Surface $|\vec{E}|$ from SUPERFISH and SuperLANS near the equator.

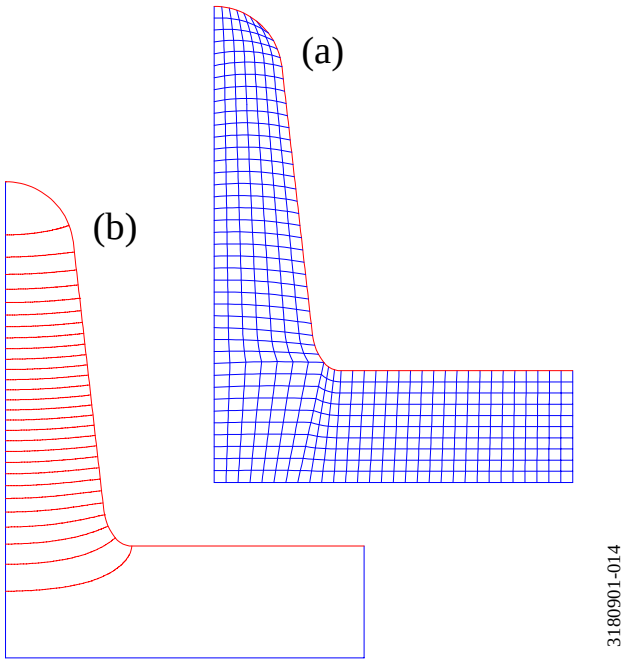

Figure 4. SuperLANS (a) mesh and (b) $\vec{E}$ field lines for an APT $\beta_g = 0.64$ single-cell cavity. The axial symmetry and left-right mirror symmetry are used to simplify the calculation, so that only one quadrant of the cavity is needed.

be due to our simple-minded way of getting $\vec{E}$ from the $\vec{H}$ values on the triangular mesh of SUPERFISH, or due to SUPERFISH problems that have been corrected in the most recent versions (we used SUPERFISH v4.12, which is several years old).

4 SIMULATION RESULTS

We will discuss the multipacting simulations for one shape in detail, and then compare the results for all of the 6 shapes shown in Figure 1.

4.1 *Example: $\beta = 0.64$ APT Cavity*

For 2 eV secondaries emerging normal to surface, the simulations indicate a band of possible multipacting for $E_p = 17$ to 24 MV/m (Figure 5, black region). The time between emission and impact for this band is half of 1 RF period, consistent with first-order 2-point multipacting. As E_p varies across the band, the start time, the impact location, and the impact energy vary with it (Figure 6).

As can be seen in Figure 6c, the impact energy increases as we increase K_i; for $K_i < 2$ eV, no multipacting is predicted. For $\alpha_i \neq 0$, K_f increases further ($\alpha_i > 0$) or multipacting is no longer sustained ($\alpha_i < 0$).

Some of the predicted trajectories are shown in Figure 7: the prediction is for 2-point multipacting very close to the equator. Soft multipacting barriers of this type were seen in LEP [17], CEBAF [12], and Milano [18] cavities.

4.2 *Other Cell Shapes*

Two-point multipacting at the equator is predicted for all 6 cavity types. The qualitative features are the same as for the APT $\beta_g = 0.64$ cavity. Figure 8 shows the predicted E_p ranges and corresponding K_f ranges for the each of the cell shapes for one combination of K_i and α_i. Simple scaling laws indicate that the local $\vec{B}$ field for a multipacting band should be proportional to the frequency; the differences in frequency and in the ratio of E_p to $\vec{B}$ at the equator between the different cavities explain the trends of Figure 8a to within about $\pm 3\%$. The impact energies are always < 40

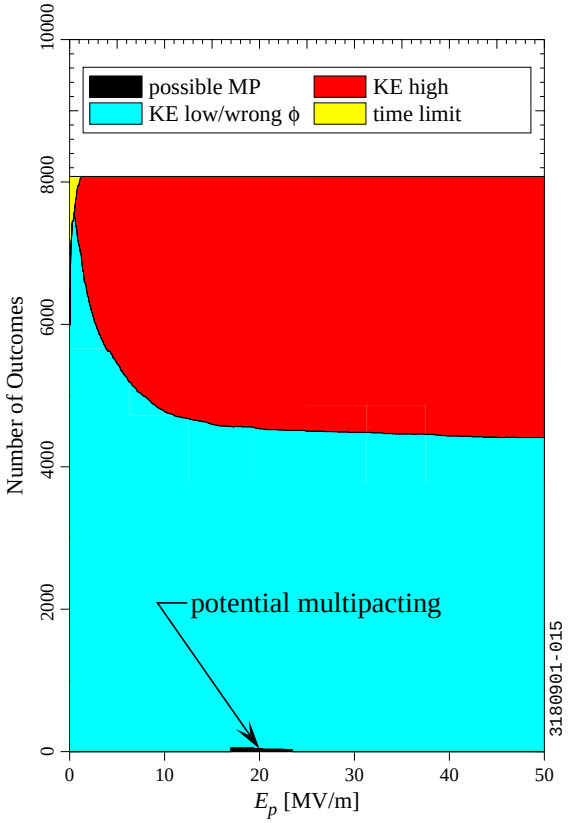

Figure 5. "Pie chart" for multipacting in the APT $\beta_g = 0.64$ cavity (in the case of $K_i = 2$ eV and $\alpha_i = 0$). For the majority of initial conditions, the simulation is ended when the K_f falls below 20 eV; for most other cases, K_f ultimately exceeds 3 keV. There is one multipacting band (black region at bottom).

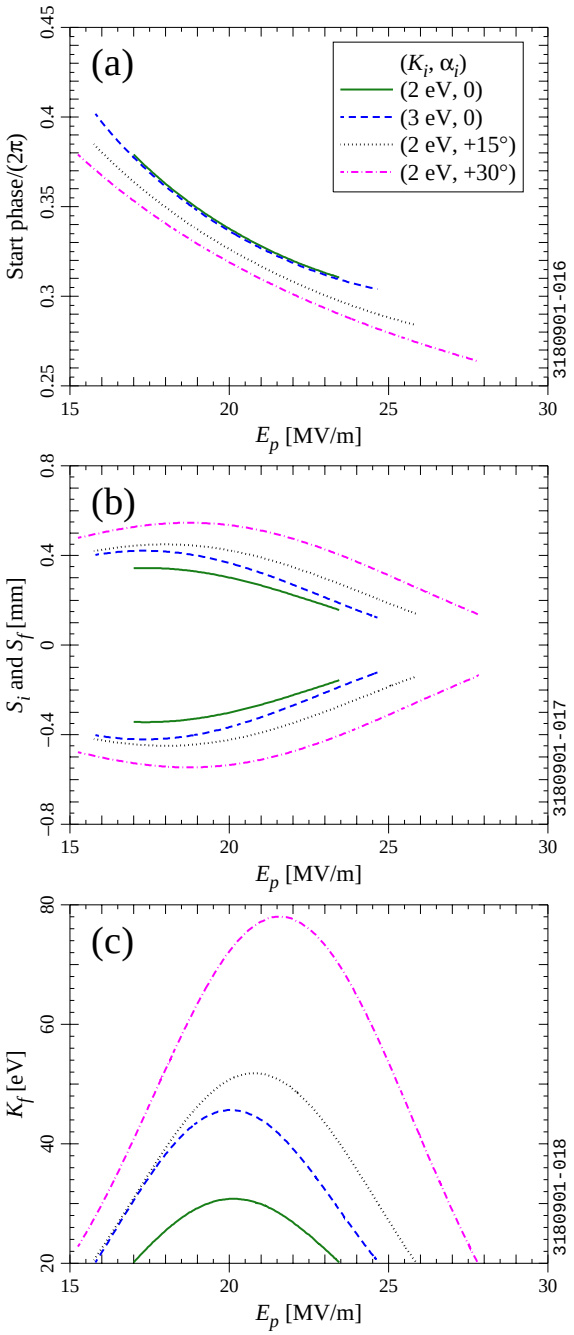

Figure 6. (a) Starting phase, (b) emission and impact location, and (c) impact kinetic energy for the multipacting band in the APT $\beta_g = 0.64$ cavity. The 4 combinations of K_i and α_i which produce multipacting are shown.

eV, so we do not expect any hard barriers. We do expect soft barriers if the initial SEY is high. Since $K_f < K_p$, we do not expect any dependence on α_f.

There is one interesting feature for the $\beta_g = 0.81$ and $\beta_g = 0.82$ cavities: for $K_i = 2$ eV and $\alpha_i = +30°$, another band of first-order 2-point multipacting is predicted at higher field ($E_p = 39$ to 45 MV/m for the APT cavity, $E_p = 56$ to 65 MV/m for the SNS cavity), with K_f up to about 120 eV. We still expect soft barriers, since $\alpha_i = +30°$ is an unlikely angle. This band does not show up for other

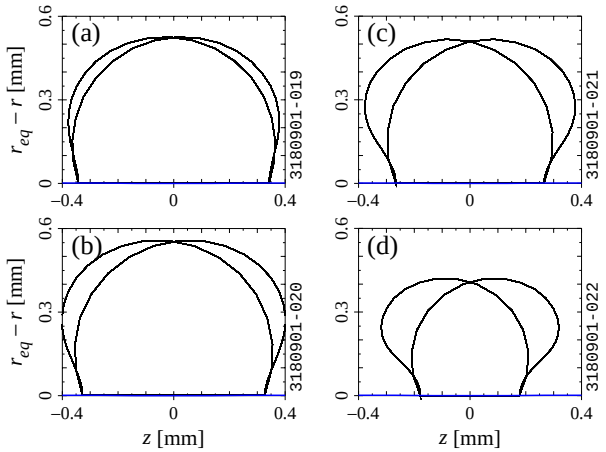

Figure 7. Trajectories in the APT $\beta_g = 0.64$ cavity for selected E_p values in the dominant multipacting band (in the case of $K_i = 2$ eV and $\alpha_i = 0$). The E_p values are (a) 17, (b) 19, (c) 21, and (d) 23 MV/m. Generations 31 through 41 of the secondary electrons are shown; the different generations follow the same orbit very closely.

combinations of K_i and α_i or in the lower-β cavities.

For the RIA $\beta_g = 0.47$ cavity, the simulations indicate that there is some possibility of multipacting across the gap of the cell at low field. Fourth-order and fifth-order multipacting (2-point in both cases) are predicted for $E_p = 0.45$ MV/m and 0.55 MV/m, respectively. The impact energies are about 2.2 keV and 1.2 keV, with $\alpha_f \approx 0$. In the simulations, the orbits are not completely stable—after many generations of secondary electrons (sometimes as many as 72), the multipacting condition can no longer be sustained. This does not guarantee that the multipacting could not be sustained in reality. On the other hand, it is unlikely that the initial conditions would be found: only a few electrons out of $\sim 10^6$ combinations produce multipacting orbits. Thus, we do not expect hard barriers.

5 DISCUSSION

5.1 *Comparison with RF Tests*

As indicated in Table 2, RF tests on APT, SNS, and RIA prototypes show no problems with multipacting. Prototypes for 5 out of 6 cell shapes have been tested. It is worth noting that an enlarged beam tube is planned for some of the cavities in order to increase the input coupling. Multipacting was seen and predicted for a single-cell cavity with one enlarged beam tube [18]. However, no multipacting was seen in multi-cell cavities with enlarged beam tubes, 4 multi-cells of the APT $\beta_g = 0.64$ type and 2 multi-cells of the SNS types having been tested [4, 5].

5.2 *Comparison with Other Simulations*

Our results for the SNS/RIA cavities are roughly consistent with those of P. Ylä-Oijala [13, 14], which predict first-order 2-point multipacting at a somewhat higher field level; the results for higher orders do not agree well, but all of the simulations predict soft barriers.

Comparing the above predictions to simulations for a

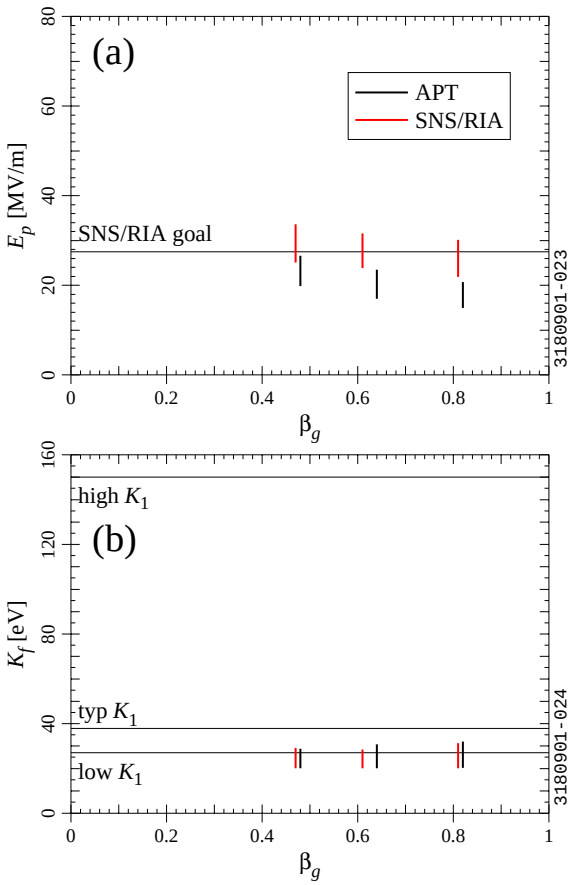

Figure 8. Predicted ranges of (a) field level and (b) impact energy for the dominant multipacting band in each of the 6 cell shapes (in the case of $K_i = 2$ eV, $\alpha_i = 0$).

Table 2. RF tests of medium-β cavities.

APT Cavities					
β_g	Cells	Number tested	max E_p [MV/m]	MP seen?	Ref
0.48	1	2	43	no	[3]
0.64	1	2	38	no	[3]
	5	6	41	no	[4]
SNS/RIA Cavities					
β_g	Cells	Number tested	max E_p [MV/m]	MP seen?	Ref
0.47	1	2	46	no	[6]
0.61	6	1	43	no	[5]
0.81	6	1	39	no	[5]

standard (center cell geometry) CEBAF single-cell cavity, the results are roughly consistent. The first-order 2-point multipacting band occurs at higher field, as expected, and the impact energies are slightly higher. The band occurs for more combinations of K_i and α_i. As for the highest-β APT and SNS cavities, a second first-order 2-point barrier is predicted at high field (for $\alpha_i = +30°$ and $K_i = 2$ eV only). Thus, we expect the soft barriers in the lower-β cavities to be slightly less severe than for the CEBAF case.

6 CONCLUSION

We have simulated multipacting in 3 cavity shapes for APT and 3 other shapes for SNS/RIA, in the range of $0.47 \leq \beta_g \leq 0.82$. The simulations indicate a soft multipacting barrier at high field, but predict no hard barriers. The predicted behaviour is similar for all 6 cavities, in spite of the differences in shape. Only single-cell cases have been simulated so far; we do not expect major differences in the multipacting behaviour of multi-cell cavities. Enlarged beam tubes may be worth further study, however.

The predictions are consistent with the RF tests on single- and multi-cell prototype cavities for APT and SNS, and single-cell prototypes for RIA. For all of the prototypes, the design field levels were exceeded, and no multipacting was reported.

We thank our colleagues, particularly G. Ciovati, T. Grimm, P. Kneisel, J. Knobloch, H. L. Phillips, and T. Tajima, for useful discussions and comments. D. Myakishev, V. Yakovlev, and S. Belomestnykh provided valuable help with SuperLANS. We thank K. C. D. Chan and R. C. York for supporting these studies.

Our bright memories of the 10th SRF Workshop are dimmed by the shadow of subsequent events. May we never forget the nightmare of 11 September 2001. And may we always remember the dream of common understanding across cultural and ideological boundaries, which brought us together for this workshop.

REFERENCES

[1] C. M. Lyneis *et al.*, *Appl. Phys. Lett.* **31**, p. 541 (1977).
[2] H. Padamsee *et al.*, *IEEE Trans. Magn.* **13**, p. 346 (1977).
[3] W. B. Haynes *et al.*, in *Proc. 8th Workshop RF Supercond.*, LNL-INFN (Rep) 133/98, 1998, p. 523.
[4] T. Tajima *et al.*, "Developments of 700-MHz 5-cell Superconducting Cavities for APT," presented at the 2001 Particle Accelerator Conference.
[5] G. Ciovati *et al.*, "Superconducting Prototype Cavities for the Spallation Neutron Source (SNS) Project," *ibid.*
[6] C. C. Compton *et al.*, "Niobium Cavity Development for the High-Energy Linac of the Rare Isotope Accelerator," *ibid.*
[7] Kenneth G. McKay, in *Advances in Electronics*, Volume I, Academic Press, New York, 1948, p. 65.
[8] O. Hachenberg & W. Brauer, in *Advances in Electronics and Electron Physics*, Volume XI, Academic Press, New York, 1959, p. 413.
[9] Roger Calder, Georges Dominichini, & Noël Hilleret, *Nucl. Instrum. Methods Phys. Res. B* **13**, p. 631 (1986).
[10] H. Padamsee & A. Joshi, *J. Appl. Phys.* **50**, p. 1112 (1979).
[11] Frank L. Krawczyk, these proceedings.
[12] J. Knobloch, W. Hartung, & H. Padamsee, in *Proc. 8th Workshop RF Supercond.*, LNL-INFN (Rep) 133/98, 1998, p. 1017.
[13] D. Barni *et al.*, Tech Note JLab-TN-01-014, Jefferson Lab, Newport News, VA (2001).
[14] G. Ciovati & P. Kneisel, private communication.
[15] K. Halbach & R. F. Holsinger, *Part. Accel.* **7**, p. 213 (1976).
[16] D. G. Myakishev & V. P. Yakovlev, in *Proc. 1995 Part. Accel. Conf.*, IEEE Publishing, Piscataway, NJ, 1996, p. 2348.
[17] W. Weingarten, in *Proc. 2nd Workshop RF-Supercond.*, CERN, 1984, p. 551.
[18] G. Devanz, in *Proc. 7th Eur. Part. Accel. Conf.*, European Physical Society, Geneva, 2000, p. 1366.